

TrajGEOS: Trajectory Graph Enhanced Orientation-based Sequential Network for Mobility Prediction

Zhaoping Hu⁺, Zongyuan Huang⁺, Jinming Yang, Tao Yang, Yaohui Jin*, *Member, IEEE*, Yanyan Xu*

Abstract—Human mobility studies how people move to access their needed resources and plays a significant role in urban planning and location-based services. As a paramount task of human mobility modeling, next location prediction is challenging because of the diversity of users’ historical trajectories that gives rise to complex mobility patterns and various contexts. Deep sequential models have been widely used to predict the next location by leveraging the inherent sequentiality of trajectory data. However, they do not fully leverage the relationship between locations and fail to capture users’ multi-level preferences. This work constructs a trajectory graph from users’ historical traces and proposes a Trajectory Graph Enhanced Orientation-based Sequential network (TrajGEOS) for next-location prediction tasks. TrajGEOS introduces hierarchical graph convolution to capture location and user embeddings. Such embeddings consider not only the contextual feature of locations but also the relation between them, and serve as additional features in downstream modules. In addition, we design an orientation-based module to learn users’ mid-term preferences from sequential modeling modules and their recent trajectories. Extensive experiments on three real-world LBSN datasets corroborate the value of graph and orientation-based modules and demonstrate that TrajGEOS outperforms the state-of-the-art methods on the next location prediction task.

Index Terms—Human mobility, Next location prediction, Graph neural networks, Trajectory graph, Attention mechanism

I. INTRODUCTION

Human mobility prediction is of great importance to numerous applications, including traffic scheduling [1], [2], electric vehicle charging management [3], urban planning [4], [5], and decision-making during large-scale emergency events [6]. Due to the deep-rooted regularity of people’s daily mobility [7], mobility modeling is scientifically possible, and numerous research fields have emerged in the past decade [8]. Besides, the increasing prevalence of mobile phones, GPS services, and digital maps contribute to the surge of location-based social networks (LBSNs) such as Foursquare, Gowalla, Yelp, etc. User-generated content in LBSNs contains not only spatial and

temporal stamps of activity but also contextual information. As the explosive growth of LBSNs made the activity data of millions of users [9] more accessible, it also brought great convenience to human mobility prediction tasks, especially for next location prediction.

As an important task of human mobility modeling [10], next-location prediction aims to predict the most possible location an individual user is going to visit. Most current research utilizes sequential models to capture users’ behavioral patterns and deduce their preferences, due to the inherent sequentiality of human mobility actions. These conventional approaches tend to employ vanilla sequential models, compounded with augmented spatial-temporal features, such as distance-matrix, to investigate behavioral patterns from massive historical trajectories. With the advancement of deep learning, recurrent neural networks (RNNs) have gained extensive acceptance for capturing sequential dependencies in next-location prediction tasks. To further make full use of spatial-temporal information, researchers have designed novel gate mechanisms [11] and introduced additional spatial-temporal features [12]–[16] to RNNs. Advanced techniques such as attention mechanism [17], [18] and transformer [19]–[21] were also applied to users’ preference modeling with their historical sequences.

The sequential modeling approaches provide critical insights into the next-location prediction problem, and experiments on real-world datasets confirmed their effectiveness. There are, however, two intractable drawbacks to these approaches. (i) They insufficiently explore the relationship among diverse locations. As Figure 1 (a) shows, there are many records of movements between the amusement park and the restaurant, which implies that they may be geographically close and have similar contexts. Yet, despite most sequential models learning the behavior of individual users, they fail to learn the global relation across different locations, which is crucial for downstream prediction tasks. (ii) How to effectively incorporate all historical trajectories to model mobile behavior is another critical issue for most existing models. It’s difficult for vanilla sequential models to capture long-term transition patterns with all historical trajectories.

Towards these issues, in this paper, we propose TrajGEOS, a trajectory graph enhanced orientation-based sequential network for mobility prediction. First, to capture the global relation between locations, we construct a large trajectory graph that aggregates all historical mobility sequences of users and applies a hierarchical graph learning approach to

Z. Hu, Z. Huang, J. Yang, Y. Jin, Y. Xu are with the MoE Key Laboratory of Artificial Intelligence and AI Institute, Shanghai Jiao Tong University, Shanghai 200240, China. E-mail: {zhaopinghu, herozen, yangjm67, jinyh, yanyanxu}@sjtu.edu.cn.

Tao Yang is with Shanghai Transportation Information Center, Shanghai Urban-Rural Construction and Transportation Development Research Institute, Shanghai 200032, China. E-mail: yangtaocoolboy@163.com

⁺ Equal contribution.

* Corresponding authors.

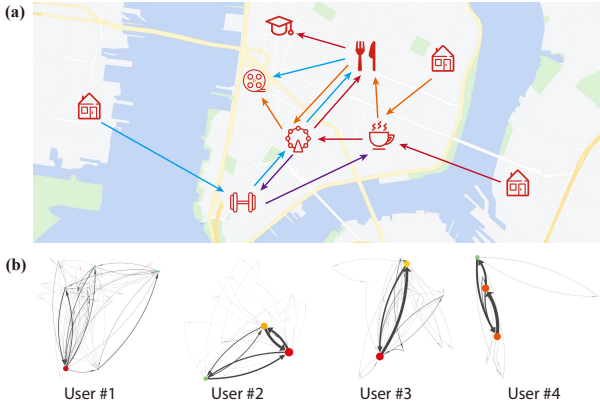


Fig. 1. (a) Implicit relationship between locations. (b) Sample users' trajectory graphs built from their historical check-in data.

generate location and user representations that contain spatial and contextual relations. These representations serve as important supplements to trajectory encoding in the sequential module. Our model incorporates next-visit category prediction as an auxiliary task, enabling it to access additional features that contain categorical information when modeling location trajectories. Besides, to better capture the user's mobility patterns and preferences, we design a next-location predictor that integrates long-term, short-term, and mid-term preferences (multi-preferences). Users' long-term preferences come from a location-weighted readout of the individual trajectory graph like Figure 1 (b) shows, and short-term preferences are drawn from the trajectory sequences within the current week. For the mid-term preference, we design an orientation module that utilizes position embedding and attention mechanism based on their trajectories over the past two weeks. The implementation of this work will be released after publication.

Our contributions can be summarized as follows:

- We design a hierarchical graph convolution approach to process the global trajectory graph. The lower convolution is applied to obtain the location embedding, while the upper convolution is applied to user-specific trajectory subgraphs to derive user representations. This structure enables further exploration of both location relationships and long-term preferences among users within their historical trajectories.
- We propose the TrajGEOS model, which captures users' multi-preferences, including long-, mid-, and short-term transition patterns, to leverage all historical records more effectively. The final predictor outputs the next location based on the user's multi-preference derived from their entire historical records.
- We conduct extensive experiments on three real-world location-based social networks (LBSNs) check-in datasets, and further confirm the effectiveness of our model through ablation experiments and visualization analyses.

II. RELATED WORK

A. Next location prediction

Current next location prediction methods mainly focus on the temporal patterns of the historical trajectory when predicting an individual's next movement. Related approaches can be classified into two categories: traditional methods and deep learning methods. Traditional methods are mostly pattern-based [22]–[24] or machine-learning based [25]–[30]. For instance, FPMC [22] adds user-personalized transition matrices and FPMC-LR [23] adds an additional localized constraint to capture users' transition patterns. [24] developed a naive Bayesian-based method combined with geographical influence to recommend the next location. With the development of matrix factorization-based methods in recommender systems, some researchers incorporate additional geographical and social influence [25], [26] or spatial clustering constrain [27] into the matrix factorization method to recommend the next place for users. The metric embedding method can better model the sequential transition with the strategy of representing each item as a single point in the latent space. So some works incorporate individuals' preference [28], category, and region information [29] to the metric embedding method and predict users' next locations. These traditional approaches are limited to feature engineering, which usually requires domain knowledge, making it difficult to construct the relationships between unstructured features from multi-format data.

Since the user trajectory data in LBSN naturally has a sequential structure, most deep learning methods use sequential models such as recurrent neural networks to capture mobility patterns. Some researchers also incorporate additional tricks, including attention mechanism [14], [17], [18], [31], [32] and flashback [13], to enhance the models and make full use of data sparsity. [12], [14], [33] add additional spatial-temporal influences and geographical relations to RNN, which help the model capture patterns in historical trajectory data. [31] proposed long and short-term modules to learn preferences, and [34] incorporate additional personalized weights for individualized recommendation. STGCN [11] designed a new LSTM with additional gate mechanisms to capture spatial-temporal features. STAN [18] and GeoSAN [32] exploit additional geographical and temporal information to predict the next location based on self-attention networks. Considering the geographical impact on location prediction, DIG [35] disentangles the geographical and user interest factor, utilizing a geo-constrained negative sampling strategy and soft-weighted loss function. SSDL [36] disentangle time-invariant and time-varying factors in human mobility patterns, utilizing trajectory augmentation techniques to mitigate data sparsity, and incorporating a POI-centric graph structure to capture heterogeneous collaborative signals from historical check-ins. CSLSL [37] integrates causal structures and spatial constraints to explicitly modeling the decision logic of human mobility and ensuring consistency between predicted and actual spatial distributions. Graph-based methods for next location prediction have garnered significant attention in recent years. These approaches leverage the structural relationships between locations, providing a powerful framework for understanding

and forecasting human mobility patterns. In the following subsection, we will provide a detailed overview of these methods.

B. Graph learning in mobility prediction

Since graph convolution neural networks emerged as an innovative method to model structured graph data, graph learning approaches have attracted extensive attention and have been widely used in different tasks. Point of interest (POI) recommendation is a usual format of next location prediction that is closely related to the recommendation task. Some recent work on the next POI recommendation leverages the graph embedding method to enhance their models with geospatial information that can be used in downstream prediction tasks. For instance, GE [38] uses POI-POI, POI-Region, POI-Time, and POI-Word bipartite graphs to capture different paradigms and make recommendations for users' next POI. DYSTAL [39] jointly learns the embedding of users and locations from three graphs, i.e., POI-POI, user-POI, and user-user, and excavates spatial-temporal patterns based on historical trajectories; also, it designs a dynamic factor graph to capture the different factors from the network embedding module. The GETNext model [19] combines graph neural network technique and transformer [40] structure to predict the next location. It uses a unified graph constructed of check-in sequences to generate the embedding of locations, and this graph construction method reflects the global transition patterns of all users explicitly. Graph-Flashback [41] introduces a Spatial-Temporal Knowledge Graph and integrates both spatiotemporal information and user preferences to explicitly learn weighted POI transition graphs. STHCN [42] leverages a hypergraph to capture both intra-user and inter-user trajectory information and incorporates a hypergraph transformer to effectively integrate spatio-temporal data. MTNet [43] introduces a novel "Mobility Tree" structure to capture users' check-in patterns across multiple time slots, enabling personalized next POI recommendations by learning specialized behavioral preferences for different temporal periods.

For the graph learning module, the construction of a graph is of great importance to the determination of what additional information to provide to downstream tasks. A user-POI graph, for example, can reveal users' historical activities, while a user-user graph usually contains the social network in a group. In our TrajGEOS model, we construct a global trajectory graph based on all users' historical check-in data and add contextual information as node features. By using hierarchical graph convolution, our graph learning module can provide additional location features and user preferences for downstream predictors.

III. PROBLEM FORMULATION

Let $U = \{u_1, u_2, \dots, u_N\}$ be a set of users, $L = \{l_1, l_2, \dots, l_M\}$ be a set of locations and N, M are the total number of users and locations in a given dataset, respectively. Each location $l_i \in L$ is associated with a tuple (c_i, lat_i, lon_i) that contains location category (e.g., shopping mall and restaurant), latitude and longitude. Based on these basic concepts, we hereafter introduce several key definitions used in this paper.

Definition 3.1 (Record). Record r_i^k is a 2-tuple (l_i^k, t_i^k) , representing user (u_i) 's visited location l_i^k at time t_i^k , where $u_i \in U$ and $l_i^k \in L$.

Definition 3.2 (Individual trajectory). The trajectory of user u_i is a sequence $R_i = [r_i^1, r_i^2, \dots, r_i^T]$ that contains all historical check-in records. Due to the sparsity of users' check-in data, the record timestamp in trajectory records is uneven and there is a large time gap in most trajectory records.

In data preprocessing, we split the trajectory R_i of every user u_i into a set of sub-trajectories, that is, $R_i = S_i^1 \oplus S_i^2 \oplus \dots \oplus S_i^{SN_i}$ where \oplus denotes concatenation, S_i^k is u_i 's k -th sub-trajectory, SN_i is the number of sum sub-trajectories for user u_i . The length of sub-trajectory may vary and each one contains the user's check-in within a time window. In this paper, we segment user's trajectory using a weekly time window as people's behavior may follow a weekly periodicity. We then split data at the user level by assigning the first 80% sub-trajectories of each user into the training set and the remaining sub-trajectories into the test set, denoted as R_i^{train} and R_i^{test} , respectively.

Definition 3.3 (Global trajectory graph). Global trajectory graph G with M nodes is a directed graph constructed of all users' trajectories $\{R_1^{train}, R_2^{train}, \dots, R_N^{train}\}$. $V = \{v_1, v_2, \dots, v_M\}$ is node set with size $|V|$ equals to the size of location set $|L|$. And $\forall v_i \in V$ in the trajectory graph represents an actual location $l_i \in L$. In the edge set $E = \{e_{i \rightarrow j}, e_{i \rightarrow j}, \dots\}$, $e_{i \rightarrow j}$ represents a directed edge from v_i to v_j , indicating the transition from location l_i to location l_j . $e_{i \rightarrow j}$ is associated with the distance between these two locations, the sum of transition numbers, and the corresponding 24-hour flow data calculated from training data.

The goal of the next location prediction is to predict where user u_i is most like to visit next, by learning from his historical trajectories. Based on the above definitions, this task can be formally described as predicting user u_i 's next location l_i^{T+1} based on the current trajectory $S_i^p = [r_i^t, r_i^{t+1}, \dots, r_i^T]$ and the recent trajectory $\{S_i^{p-\kappa}\}$, $\kappa \in [1, \dots, p-1]$. In this paper, we set $\kappa = 2$, that is, we consider check-in records within the preceding 2~3 weeks as the recent trajectory.

IV. METHODOLOGY

A. Model Structure Overview

Figure 2 illustrates the framework of our TrajGEOS model, which consists of three key components. Firstly, we construct a trajectory graph based on the check-in records of all users in the training data and then apply hierarchical graph convolution operation to capture the embeddings of each location and each user, enriched with additional spatial and contextual information. Second, within the trajectory embedding module, we utilize the embedding layer to encode the contextual information of the user's historical check-in locations. By incorporating additional embeddings from our graph learning module, we can obtain encoded trajectory sequences. Thirdly, in the prediction module, we design a multi-task predictor that employs a shared GRU to capture patterns in sub-trajectories and utilizes two independent MLPs to predict the next location and category. In the following subsections, we will provide further elaboration on the TrajGEOS model.

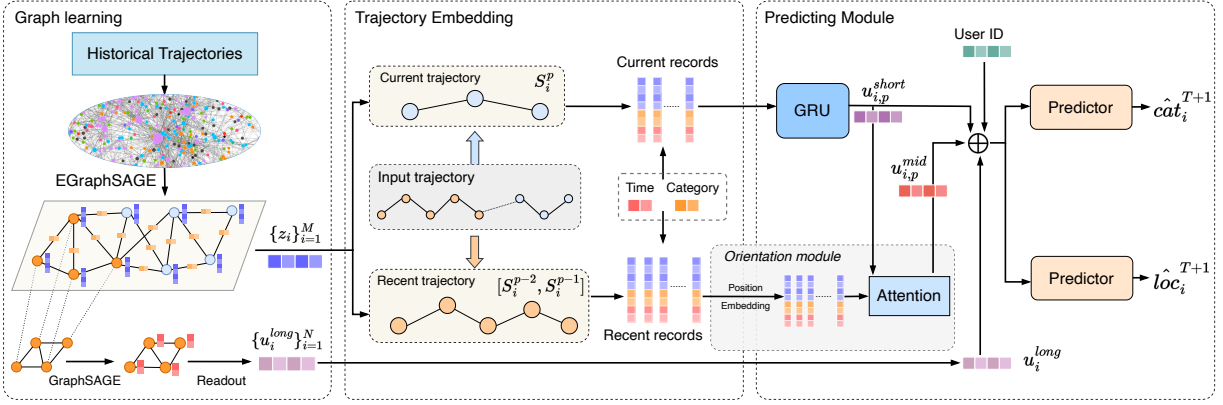


Fig. 2. The architecture of TrajGEOS. It contains three modules: graph learning module, trajectory embedding module, and prediction module.

B. Learning with Trajectory Graph

Initialization in trajectory graph. Given the trajectory graph, we first initialize its node features and edge features. The raw features of a location l_i include its identity, category c_i and coordinate (lat_i, lon_i) . That is, the initial node feature of l_i is:

$$h_i^0 = Emb(l_i) \parallel Emb(c_i) \parallel lat_i \parallel lon_i \quad (1)$$

where $Emb(l_i)$, $Emb(c_i)$ represent the embedding of location ID and the embedding of category. And $Emb(\cdot)$ represents the basic Embedding layer.

As for the initialization of edges, for every edge $e_{i \rightarrow j}$, we calculate the distance $distance_{i \rightarrow j}$ between l_i and l_j and count the sum transition numbers $trans_{i \rightarrow j}$ from l_i to l_j from all training data. Moreover, for every $e_{i \rightarrow j}$, we formulate a 24-dim flow vector $flow_i = [n_0, n_1, \dots, n_{23}]$. The k -th dim in the $flow$ of $e_{i \rightarrow j}$ represents the record number of transitions from l_i to l_j at hour k in all training data. With these features, we get the initial embedding of edge $e_{i \rightarrow j}$ like the following equation shows:

$$\mathcal{E}_{i \rightarrow j}^0 = trans_{i \rightarrow j} \parallel distance_{i \rightarrow j} \parallel flow_{i \rightarrow j} \quad (2)$$

Graph convolution on global trajectory graph. To make full use of node features and edge features in the global trajectory graph, we adopt GRAPE [44] (hereafter referred to as EGraphSAGE) as the lower graph convolution structure to learn location embeddings. EGraphSAGE not only leverages the features of neighboring nodes and edges in the process of message passing but also simultaneously updates node and edge embeddings. In global trajectory, the initial node feature includes identity, coordinates, and category (for some datasets) and the initial edge feature includes distance and flow data between locations. So we not only update the node features but also update the edge feature using the updated node features in each EGraphSAGE layer. The operation of the EGraphSAGE

layer is like the following equation shows:

$$h_{\mathcal{N}(s, \epsilon)}^k = \text{MEAN}(\sigma(\mathbf{W}_1^{k-1} \cdot \text{CONCAT}(h_s^{k-1}, \mathcal{E}_{t \rightarrow s}^{k-1}) \mid \forall t \in \mathcal{N}(s, \epsilon))) \quad (3)$$

$$h_s^k = \sigma(\mathbf{W}_2^k \cdot \text{CONCAT}(h_s^{k-1}, h_{\mathcal{N}(s, \epsilon)}^k)) \quad (4)$$

$$\mathcal{E}_{t \rightarrow s}^k = \sigma(\mathbf{W}_3^k \cdot \text{CONCAT}(\mathcal{E}_{t \rightarrow s}^{k-1}, h_t^k, h_s^k)) \quad (5)$$

where $\mathbf{W}_1^k, \mathbf{W}_2^k, \mathbf{W}_3^k$ are learnable parameters, ϵ is the edge dropout ratio in the global trajectory graph. The global trajectory graph is a complex and humongous structure that records all users' mobility traces in a specific region. Transition backbones like core metro or bus stations usually carry a large flow of human mobility. As a result, their corresponding nodes in the global trajectory graph always have large degrees. Operating graph convolution on these nodes makes these central nodes update their embedding based on numerous neighborhoods. As a result, makes it easier to over-smoothing. So we set edge dropout ratio ϵ to 0.5, which is an experiential value used in dropout layers, in our experiments to avoid complex network structure and alleviate the over-smoothing problem. s, t represent nodes v_s, v_t in graph, $\mathcal{N}(s, \epsilon)$ are the neighbor set of node v_s with edge dropout ratio ϵ , h_s^k is node v_s 's embedding in the k -th layer.

We next extract $h_i^2 \in \mathbb{R}^{d_{GI}}$ as the output of the 2-layer graph convolution on the global trajectory graph, where d_{GI} is the dimension of node embedding in the graph learning module. Then we concatenate h_i^2 with the initial node feature h_i^0 and feed the concatenated vector into a dense layer utilized in [19]. The output can be denoted as:

$$z_i = \sigma(\mathbf{W}_4[h_i^2 \parallel h_i^0] + b) \quad (6)$$

where \mathbf{W}_4 and b are trainable parameters. We regard $z_i \in \mathbb{R}^{d_{GI}}$ as the final embedding of location l_i . Now that after graph learning, we can collect the embeddings of all locations, and then have the embedding matrix $\mathbf{Z} \in \mathbb{R}^{M \times d_{GI}}$ as the location feature for downstream modeling.

Graph learning on user's trajectory graph. To capture the user's historical mobility patterns, we further apply graph convolution on user subgraphs and calculate the subgraphs' readout as the user's stable long-term preference. More specifically, the calculation consists of the following steps. Firstly,

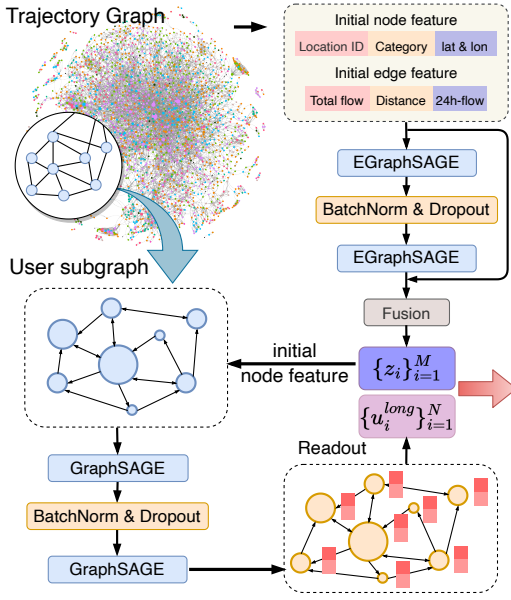


Fig. 3. Hierarchical graph convolution in the graph modeling module.

for a specific user, say u_i , we extract his subgraph G_i from the trajectory graph based on his historical check-in records R_i^{train} . In G_i , the node set is V_i , corresponding to u_i 's visited location set L_i , the edge set is E_i . The initial node embedding of $v_j \in V_i$ is the z_j obtained from the global location embedding matrix \mathbf{Z} . Next, we use 2-layer GraphSAGE [45] to update node embeddings in the user's trajectory graph and finally get $\{h_{i,j}^2\}$ where $l_j \in V_i$ as location embeddings unique to user u_i . For user u_i , the updating of node embeddings in the GraphSAGE layer is like the following shows:

$$h_{i,\mathcal{N}(s,\epsilon)}^k = \text{mean}(\{h_t^{k-1}, \forall t \in \mathcal{N}(s,\epsilon)\}) \quad (7)$$

$$h_{i,s}^k = \sigma(\mathbf{W}_5^k \cdot \text{CONCAT}(h_{i-1,s}^{k-1}, h_{i,\mathcal{N}(s,\epsilon)}^k)) \quad (8)$$

where \mathbf{W}_5^k is a trainable parameter, while s, t, ϵ have the same meaning as in the equations of EGraphSAGE layers. $h_{i,s}^k$ represents the embedding of node v_s , which is unique to user u_i , in the k -th layer. It is worth noting that the graph convolutions on user subgraphs do not affect the node embeddings in the global trajectory graph.

Then, we calculate the visiting weight for every location within the user's trajectory subgraph. Assume that user u_i 's visiting set is V_i and $\eta_{i,j}$ is the number of records user u_i visited location l_j . The sum of records of user u_i is $RN_i = \sum_{l_j \in V_i} \eta_{i,j}$. For user u_i , the visiting weight of the location l_j is $w_{i,j} = \eta_{i,j}/RN_i$.

The visiting weight-based readout of user u_i 's trajectory subgraph is calculated with the following formula:

$$u_i^{long} = \sum_{l_j \in V_i} w_{i,j} \cdot h_{i,j}^2 \quad (9)$$

where $h_{i,j}^2$ is the embedding of location l_j unique to user u_i . We regard the user embedding u_i^{long} , which is obtained from the user's trajectory graph, as user u_i 's long-term preference, and utilize it in the downstream prediction task. The detailed

structure of the graph learning module is shown in Figure 3, and the whole process of the graph learning task is formally shown in Algorithm 1.

C. Embedding and capturing of trajectory

We encode the raw trajectory records into embedding sequences and employ sequential models to capture transition patterns. This subsection presents the trajectory captures for the downstream sequential model.

Embedding layers. Every data record r_i^k for user u_i is a 2-tuple (l_i^k, t_i^k) , including location id l_i^k , visiting time t_i^k , and the location category c_i^k associated with l_i^k . We use basic embedding layers to encode user ID and category ID information. These id-based embeddings play an important role in distinguishing different check-in records. The visiting time t_i^k includes both visiting-weekday and visiting-hour information, and some check-in records might be periodic in time. Thus, we use Time2Vec [46] to model the periodicity and get $Time2Vec(t_i)$ for every timestamp. Additionally, $Emb(u_i)$, $Emb(c_i)$, $Time2Vec(t_i)$ are used to represent the embedding of user u_i , category c_i , and time t_i .

Trajectory Embedding. As we have introduced in Section III, we leverage the user's historical trajectory from the past three weeks to predict their next visiting location instead of relying on their entire historical trajectory. Here we do not make a strict distinction but uniformly use 'trajectory' to refer to the historical trajectory data used in prediction. As previously mentioned, every user's trajectory is a sequence of check-in records that include user id, location id, category id, and visiting time. Assume user u_i has one record r_i^k that visited location l_j at time t_j , where c_j is the category of location l_j . Then we can embed this single record based on the embeddings presented above:

$$Q(r_i^k) = z_j || Emb(c_j) || Time2Vec(t_j) \quad (10)$$

Where z_j , which represents the location identity, is the output of lower graph convolution module, $Emb(c_j)$ and $Time2Vec(t_j)$ are the embedding of location category and visiting time. So the encoded trajectory $Q(S_i^p)$ is:

$$Q(S_i^p) = [Q(r_i^k), Q(r_i^{k+1}), \dots] \quad (11)$$

Where the actual trajectory is $S_i^p = [r_i^k, r_i^{k+1}, \dots]$.

To better model the travel patterns of users across different historical periods, we partition every user's historical trajectory into two segments. Specifically, we define the check-in records within the latest week as the current trajectory and those within the preceding 2-3 weeks as the recent trajectory.

We utilize GRU to directly model the user's encoded current trajectory and interpret its output as the user's short-term preference for the next movement. In downstream prediction, the output of GRU not only directly contributes to the prediction, but also plays a role in calculating the user's mid-term preference as a query, which will be further elaborated in the next subsection.

D. Predicting Module

1) *Orientation Module*: Although long- and short-term preferences are commonly utilized in many existing methods [17], [31], [33], we propose that incorporating the user’s recent historical trajectory is crucial for complementing their travel preference information. Therefore, we design an orientation module that leverages encoded recent historical trajectory sequences and the outputs of GRU to capture the user’s mid-term preferences.

Recent historical trajectory. Assume the target next location of user u_i is l_i^{T+1} and u_i ’s latest check-in record is located in sub-trajectory $S_i^p = [r_i^k, r_i^{k+1}, \dots, r_i^T]$, which is regarded as the current trajectory. We select the recent sub-trajectory $[S_i^{p-2}, S_i^{p-1}]$ as the recent historical trajectory for u_i to predict the next location l_i^{T+1} . Because we split trajectory by week in this paper, the recent historical sequence of user u_i actually corresponds to his historical records in the preceding 2~3 weeks.

Position Embedding. We encode the user’s recent historical trajectory in the same format as input sequences of GRU and get corresponding encoded sequences. Then we add positional embeddings to these encoded recent historical trajectories. We use sine and cosine functions proposed in transformer [40]: With the incorporation of additional position embedding, the following module can grasp the relative positions in encoded recent historical trajectories.

Subsequently, we leverage the attention mechanism to compute the user’s mid-term preference based on the enforced encoded trajectories with position embedding and GRU module outputs. Assume $u_{i,p}^{short}$ is the output of GRU when the input is S_i^p , and the user u_i ’s encoded recent trajectory is $\{Q(r_i^j)\}$, where $r_i^j \in [S_i^{p-2}, S_i^{p-1}]$. The output of orientation module $u_{i,p}^{mid}$ is defined as:

$$\beta_j = MLP \left(Q(r_i^j) \parallel u_{i,p}^{short} \right) \quad (12)$$

$$u_{i,p}^{mid} = \sum_{j=1}^k \frac{\exp(\beta_j)}{\sum_{l=1}^k \exp(\beta_l)} \cdot Q(r_i^j) \quad (13)$$

We regard $u_{i,p}^{mid}$ as the user u_i ’s mid-term preference when his current trajectory is S_i^p and use it for the next location prediction task.

2) *Multi-task learning in TrajGEOS*: We design a multi-task learning strategy for TrajGEOS like Figure 2 shows. The next category prediction task is regarded as an auxiliary task, which shares the same GRU outputs with next location prediction task and utilizes another MLP to predict the next category.

Predicting next category and location For user u_i , set $Emb(u_i)$ as the encoded user id generated by basic embedding layer. Assume u_i ’s current trajectory is S_i^p . Then user u_i ’s preference ϕ_i^T used for the prediction of next category cat_i^{T+1} and loc_i^{T+1} can be represented as:

$$\phi_i^T = u_{i,p}^{short} \parallel u_{i,p}^{mid} \parallel u_i^{long} \parallel Emb(u_i) \quad (14)$$

Where $u_{i,p}^{short}$ is the output of GRU that processed u_i ’s encoded current trajectory S_i^p , $u_{i,p}^{mid}$ is the corresponding mid-

term preference generated by orientation module and u_i^{long} is user’s long-term preference from graph learning module.

We consider the next place and category prediction job as a multi-classification task, that can be formally formulated as:

$$\widehat{cat}_i^{T+1} = \operatorname{argmax} (MLP_c(\phi_i^T)) \quad (15)$$

$$\widehat{loc}_i^{T+1} = \operatorname{argmax} (MLP_l(\phi_i^T)) \quad (16)$$

Loss function. As a multi-task learning model, our loss function includes the cross entropy losses of both the next category prediction \mathcal{L}_c and the next location prediction \mathcal{L}_l . For example, the cross entropy loss of next location prediction \mathcal{L}_l is:

$$\mathcal{L}_l = - \sum_{j=1}^M y_j \log(p_j) \quad (17)$$

Where M is the dimension of loc_i^{T+1} , y_j equals to 1 only when $loc_i^{T+1} = l_j$ and p_j is the j -th dimension of $\operatorname{softmax}(loc_i^{T+1})$. The total loss of TrajGEOS is:

$$\mathcal{L} = \alpha \mathcal{L}_l + (1 - \alpha) \mathcal{L}_c \quad (18)$$

Where α is the hyperparameter that controls the weights of different tasks. In this paper, we set α to 0.7 to obtain the optimal *Recall@1* for the next location prediction task. Further details about the experiments of α can be found in Table IV.

V. EXPERIMENTS

A. Experimental Setup

1) *Datasets*.: We conduct experiments on three public check-in datasets: NYC [9], TKY [9], and Gowalla [47] in Dallas. The NYC dataset was collected from April 2012 to February 2013 in New York City, and TKY was from Tokyo during the same period. Data in Dallas consists of the public check-in data with time and location information, collected from Feb. 2009 to Oct. 2010. Records in NYC and TKY contain fields including user ID, location ID, location category ID, GPS coordinate, and timestamp. The record fields of Dallas are similar to those in NYC except that there is no category data. So we do not use category information to encode trajectories in the Dallas dataset. For all three datasets, we exclude unpopular locations and the outlier users with less than 10 records, in line with [17], [33]. Also, we merge the contiguous records with the same user and location at the same hour. After the preprocessing, we further process the data for our TrajGEOS model by splitting the user’s entire trajectory into sub-trajectories according to week. Every sub-trajectory should contain check-in records of a single user for at least two instances in a week. Additionally, every user must have at least five sub-trajectories following the setting of [17].

The baseline models have specific data input requirements, thus we utilize the source code provided by the authors for data processing. Overall, the datasets exhibit minimal differences, allowing for a meaningful comparison. Additionally, GETNext [19] and MTNet [43] cannot be applied to the Dallas dataset as it requires category information in training. The statistical information of data used by different models is shown in Table I.

TABLE I
DATASET INFORMATION

	NYC			TKY			Dallas		
	user	location	records	user	location	records	user	location	records
RAW	1,083	38,333	227,428	2,293	61,858	573,703	5,894	5,767	167,016
Processed	1,083	4,638	139,183	2,293	7,222	427,746	2,412	5,642	146,117
FPMC-D	1,083	4,638	138,099	2,293	7,222	425,450	2,412	5,642	143,704
FPMC-W	1,083	4,638	138,098	2,293	7,222	425,445	2,412	5,642	143,704
DeepMove	1,061	4,627	111,968	2,284	7,206	333,215	1,193	5,346	93,911
GeoSAN	1,073	4,611	138,229	2,289	7,209	427,157	2,300	5,357	142,980
LSTPM	1,019	4,614	121,148	2,233	7,201	395,192	954	5,366	103,664
GETNext	1,066	4,621	131,920	2,280	7,200	414,993	-	-	-
MTNet	1,066	4,621	131,920	2,280	7,200	414,993	-	-	-
TrajGEOS	1,065	4,635	131,874	2,280	7,204	414,855	1,357	5,428	118,069

2) *Baselines.*: In recent years, some effective solutions have been proposed to tackle the next location prediction problem. Here we select the following baselines for comparison:

- FPMC [22] is a Markov-based model utilizing matrix factorization to process users’ personalized transition matrix and learn individual transition patterns.
- DeepMove [17] is an attentional recurrent model using attention mechanism and GRU to capture long- and short-term transition patterns.
- LSTPM [33] uses the non-local network to model the user’s long-term preference, and leverages geo-dilated RNN to capture geographical relations among non-consecutive locations.
- GeoSAN [32] is a seq2seq model that uses attention-based networks as the encoder and decoder, and designs geography-aware negative samplers to use spatial information.
- GETNext [19] applies graph learning on trajectory graph to capture the global transition patterns among locations and leverages a transformer architecture to facilitate the prediction of users’ next movements.
- MTNet [43] introduces a novel tree structure to hierarchically describe the users’ preferences across varying temporal periods.

3) *Evaluation metrics.*: We select the two most commonly used metrics in next location prediction tasks, recall and mean reciprocal rank to evaluate models’ performances. Given a test data with m samples, $Recall@K$ and $MRR@K$ are defined as follows:

$$R@K = \frac{1}{m} \sum_{i=1}^m \mathbb{1}(rank \leq K) \quad (19)$$

$$M@K = \frac{1}{m} \sum_{i=1}^m \frac{\mathbb{1}(rank \leq K)}{rank} \quad (20)$$

where m is the number of test data, $\mathbb{1}$ is an indicator function and returns 1 if the condition is true, otherwise 0. $rank$ is the index of the true predicted location or category in the recommended order list. We finally set $K = 1, 5, 10$ for the Recall metric and $K = 10$ for MRR. For both $R@K$ and $M@K$, a larger value means better performance.

B. Main Results

Our TrajGEOS model employs a multi-task learning approach, with the primary task being next location prediction and the secondary task being next category prediction. Most baseline models except GETNext and MTNet, however, only

focus on predicting the next location without considering the category. Therefore, we first compare the performance of the next location prediction task in Table II. Furthermore, since the baseline models do not directly predict the category of user’s next location, we utilize a mapping between location and category that is derived from raw check-in data to convert their predicted location IDs into corresponding categories. We then evaluate the performance of next category prediction and present the results in Table III. The results of our models are computed through averaging across five independent runs, ensuring the stability of TrajGEOS experimental results. And we report $Recall@1$ ($R@1$), $Recall@5$ ($R@5$), $Recall@10$ ($R@10$), and $MRR@10$ ($M@10$) for all datasets.

For all datasets, our model outperforms the baseline models in the next location prediction task. In terms of $Recall@1$ in the location prediction task, TrajGEOS achieves 27.2%, 24.9%, and 13.2% in NYC, TKY, and Dallas datasets, while the $Recall@1$ values for the baseline model with the best performance are 26.4%, 23.8%, and 13.1%. Among the baseline methods, MTNet achieves superior performance in $Recall@1$ and $MRR@10$ but does not ensure optimal results in $Recall@5$ and $Recall@10$. In contrast, TrajGEOS consistently maintains a leading performance across all four evaluation metrics.

C. Ablation Study

To examine the contributions of different components in TrajGEOS, we design four ablation models:

- TrajGEOS-woGraph: eliminates the graph learning module and disregards any long-term user preferences learned from their trajectory graph.
- TrajGEOS-onlyGraph: only uses graph learning module to learn the embedding of locations in trajectory and user’s long-term preference. It does not use embedding layers to model the location category and does not use the embedding of the raw user ID.
- TrajGEOS-woShort: does not calculate the user’s short-term preference for the downstream predictor.
- TrajGEOS-woMid: deletes the orientation module and does not calculate the user’s mid-term preference for the downstream predictor.

Table II presents the results of ablation studies that focus on the location prediction task. We find that TrajGEOS-woShort has the poorest performance among the models, which means users’ short-term preferences are of great importance in modeling the transition pattern. The TrajGEOS-onlyGraph experiment reveals that the embedding of users based on their historical trajectory graphs (user’s long-term preference) cannot fully substitute for raw user ID features in distinguishing between different users. Moreover, incorporating category information from a user’s historical trajectory enhances the accuracy of predicting their next location.

D. Visualization

To intuitively compare the performance of different models, We visualize the prediction results of TrajGEOS along with the

TABLE II
RESULTS OF NEXT LOCATION PREDICTION TASK

Model	NYC				TKY				Dallas			
	R@1	R@5	R@10	M@10	R@1	R@5	Recall10	M@10	R@1	R@5	R@10	M@10
FPMC-D	0.1598	0.4581	0.5816	0.2842	0.1279	0.3575	0.4701	0.2243	0.0596	0.1653	0.2300	0.1052
FPMC-W	0.1469	0.4437	0.5788	0.2714	0.1225	0.3425	0.4565	0.2158	0.0550	0.1626	0.2275	0.1020
DeepMove	0.2007	0.4108	0.4685	0.2890	0.1605	0.3244	0.3924	0.2305	0.0905	0.1884	0.2294	0.1320
GeoSAN	0.1445	0.3886	0.5592	0.2537	0.2049	0.4557	0.5968	0.3155	0.0670	0.2065	0.2935	0.1255
LSTPM	0.2431	0.5478	0.6645	0.3714	0.2103	0.4602	0.5588	0.3155	0.1313	0.2567	0.3269	0.1842
GETNext	0.2406	0.5323	0.6220	0.3625	0.2180	0.4583	0.5550	0.3203	-	-	-	-
MTNet	0.2635	0.5445	0.6230	0.3817	0.2388	0.4816	0.5698	0.3414	-	-	-	-
TrajGEOS	0.2721	0.5740	0.6716	0.3982	0.2490	0.5043	0.5997	0.3564	0.1326	0.2646	0.3280	0.1893
TrajGEOS-woGraph	0.2622	0.5678	0.6651	0.3899	0.2017	0.4531	0.5484	0.3075	0.1071	0.2423	0.2960	0.1645
TrajGEOS-onlyGraph	0.2653	0.5540	0.6444	0.3859	0.2439	0.4936	0.5864	0.3491	0.1227	0.2411	0.2978	0.1737
TrajGEOS-woShort	0.2318	0.5434	0.6566	0.3615	0.2006	0.4666	0.5712	0.3126	0.1093	0.2462	0.3063	0.1680
TrajGEOS-woMid	0.2638	0.5693	0.6692	0.3910	0.2478	0.5054	0.6046	0.3565	0.1310	0.2665	0.3290	0.1887

other five baseline models on the datasets of NYC and TKY and also check the impact of various factors on the prediction task.

We plot Figure 4 (a) to explore the distribution of distance errors, which are calculated based on the distance between predicted top-1 locations and target locations, generated by the prediction results of the models. The cumulative distribution function (CDF) curve of the distance deviation for TrajGEOS lies above that of the baseline model, indicating that the distance deviations of TrajGEOS are concentrated in smaller values. This suggests that the predictions made by TrajGEOS are spatially closer to the ground truth, thereby demonstrating superior predictive performance.

Besides, a user's activity level greatly impacts the next location prediction task. Since the number of users' check-in records is related to their activity, we categorize users according to the number of their historical records and look into the average performance in different user groups. Results in Figure 4 (b) show that more historical records are beneficial to the modeling of a user's transition pattern. As for why some users with more than 300 records do not have a better performance, it is because there are few active users in the NYC dataset so the results can not reflect the actual performance at the group level.

To measure the complexity of users' historical trajectories, we design two indicators, 'location entropy' and 'category entropy', for historical trajectories. Assume that a set of user's visited locations is $L_u = [l_1, l_2, \dots, l_k]$ and $\forall l_i \in L_u$, η_i is the number of times the user visited the specific location l_i . The location entropy E_{loc} for this user can then be calculated as:

$$q_i = \eta_i / \sum_{l_j \in L_u} \eta_j \quad (21)$$

$$E_{loc} = - \sum_{l_i \in L_u} q_i \log(q_i) \quad (22)$$

Category entropy E_{cat} can be calculated in a similar manner on the user's historical access category collection.

To compare the performance of the models on users with different complexities, we divide the users into groups according to their location entropy and then calculate the average prediction performance of different models for each user group. The result is visualized by barplot in Figure 5 (a).

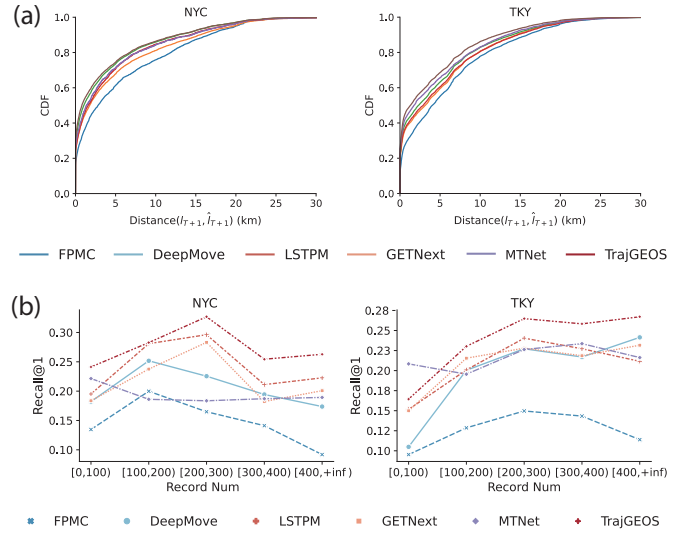


Fig. 4. (a) The cumulative distribution function of distance error (\hat{l}^{T+1}, l^{T+1}). (b) The relationship between users' record num and the predicted accuracies of their next locations.

The polyline in Figure 5 (a) corresponds to the y-axis on the right side and represents the proportion of the users belonging to different location entropy intervals in the test data for TrajGEOS.

The category of visiting location is closely related to the user's activity, which reflects some internal logic of the user's mobility behavior. So we analyzed the impact of historical category complexities on prediction accuracy. Following the manner of Figure 5 (a), we plot the prediction accuracies under different category entropies as shown in Figure 5 (b). The results show that the more complex a user's historical categories are, the more difficult it is to accurately predict his next movement.

VI. CONCLUSION

In this paper, we propose TrajGEOS, a trajectory graph enhanced orientation-based sequential model, to predict users' next locations. To capture the relationships among locations and a user's long-term preferences, we apply graph learning technology to the global trajectory graph. Also, to explore a user's recent tendency, we design an orientation module that

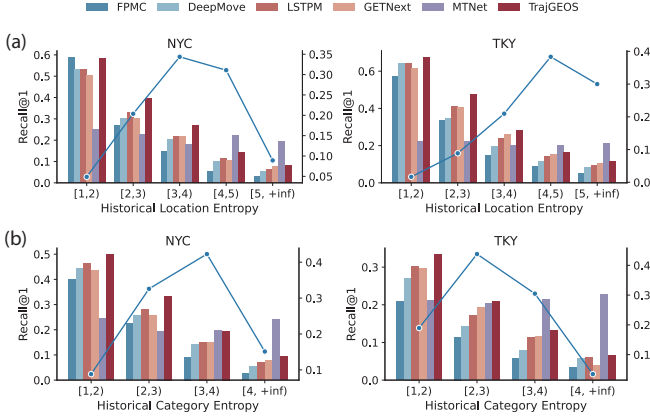


Fig. 5. (a) Relationship of historical location complexity and predicted accuracy. (b) Relationship of historical category complexity and predicted accuracy.

integrates position embedding techniques with attention mechanisms to compute their mid-term preferences. Moreover, our TrajGEOS model leverages a multi-task prediction strategy, where the next category prediction serves as an auxiliary task to enhance the next location prediction. A series of experiments on three LBSN datasets demonstrate that our proposed model outperforms all state-of-the-art models, and ablation studies also confirm the effectiveness of our model’s different components. For future work, we will verify the scalability of TrajGEOS on dense mobility datasets such as population-scale mobile phone data, and investigate whether friendship networks can contribute to the next location prediction tasks on LBSN datasets.

ACKNOWLEDGMENTS

This work was supported by the National Science Foundation of China (62102258), the Shanghai Municipal Science and Technology Major Project (2021SHZDZX0102) and the Fundamental Research Funds for the Central Universities. The computations in this paper were run on the AI for Science Platform supported by the Artificial Intelligence Institute at Shanghai Jiao Tong University.

APPENDIX A

DETAILED ALGORITHM OF GRAPH LEARNING MODULE

APPENDIX B

DETAILED EXPERIMENTAL PARAMETERS

We implement our TrajGEOS model using the Pytorch framework and Pytorch Geometric library. The dimensions of user id embedding, category id embedding, weekday embedding, and hour embedding are set to 64, 64, 16, and 16 for all datasets. The dimension of the hidden state in all GRUs is 256 and α for multi-task learning and is set to 0.7.

Settings in graph learning. We use location ID, category and GPS coordinates information to initialize the embedding for nodes in the trajectory graph. We set two 64-dim embedding layers to encode raw location ID and category data. Then

Algorithm 1: Graph learning

Input : Trajectory graph G with node set V , edge set E , location set $L = \{l_i\}_{i \leq M}$. User set U .
Output: Location embeddings $\{z_i | \forall v_i \in V\}$; User embeddings $\{u_i^{long} | \forall u_i \in U\}$;

```

1 for  $v_i \in V$  do
2    $h_i^0 \leftarrow$  initialize node according to Eq. 1 ;
3 end
4 for  $e_{i \rightarrow j} \in E$  do
5    $\mathcal{E}_{i \rightarrow j}^0 \leftarrow$  initialize edge according to Eq. 2 ;
6 end
7 for  $k = 1, 2$  do
8   Update  $\{h_i^k | \forall v_i \in V\}$  according to Eq. 3 4 ;
9   Update  $\{\mathcal{E}_{i \rightarrow j}^k | \forall e_{i \rightarrow j} \in E\}$  according to Eq. 5 ;
10 end
11  $z_i \leftarrow \forall v_i \in V$  calculate  $z_i$  according to Eq. 6 ;
12 for  $u_i \in U$  do
13    $G_i \leftarrow$  the trajectory graph of  $u_i$  ;
14    $V_i \leftarrow$  node set in  $G_i$  ;
15    $h_{i,j}^0 \leftarrow z_j, \forall v_j \in V_i$  ;
16   for  $k = 1, 2$  do
17     Update  $h_{i,j}^k$  according to Eq. 7 8,  $\forall v_j \in V_i$  ;
18      $h_{i,j}^k \leftarrow h_{i,j}^k / \|h_{i,j}^k\|_2, \forall v_j \in V_i$  ;
19   end
20    $u_i^{long} \leftarrow$  Calculate  $u_i^{long}$  according to Eq. 9 ;
21 end
22 return  $\{z_i | \forall v_i \in V\}, \{u_i^{long} | \forall u_i \in U\}$ 

```

we concatenate location embedding, category embedding, and the original latitude and longitude to generate the initial embedding for nodes. The dimension of nodes in the trajectory graph, which corresponds to the actual location, is set to 128, And the readout of each user’s trajectory graph is a 128-dimensional embedding. When it comes to graph convolution operation, we set the edge dropout ratio to 0.5 and add dropout layers with $p = 0.5$ between graph convolution layers in both the lower convolution on the global trajectory graph and the higher convolution on the user’s trajectory graph. The fusion module within the global graph convolution employs a linear layer that takes both the original location embedding and the location embedding obtained after graph convolution as input. The output embedding dimension is identical to that of the global graph convolution feature.

Optimizer and learning rate. TrajGEOS uses the Adam optimizer on all these 3 datasets. We set the learning rate to $1e-4$ for all three datasets and set the weight decay parameter to $1e-4$. More experimental settings can be found in our code.

APPENDIX C

ADDITIONAL EXPERIMENTAL RESULTS

A. Next category prediction results

Table III shows the predicted category prediction results of our model and baseline models, using the same experimental setup as Table II. Table II has proved that TrajGEOS outperforms all baseline models on the next location prediction

task, yet it does not exceed all baseline models regarding next category prediction.

TABLE III
RESULTS OF NEXT CATEGORY PREDICTION TASK

Model	NYC				TKY			
	R@1	R@5	R@10	M@10	R@1	R@5	R@10	M@10
FPMC-D	0.2191	0.5547	0.6863	0.3597	0.4292	0.6208	0.7119	0.5119
FPMC-W	0.2051	0.5419	0.6816	0.3456	0.4217	0.6085	0.7030	0.5034
DeepMove	0.2470	0.4956	0.5767	0.3527	0.3960	0.5628	0.6227	0.4687
GeoSAN	0.1738	0.4585	0.6304	0.2970	0.2543	0.5629	0.7188	0.3873
LSTPM	0.2965	0.6386	0.7538	0.4408	0.4492	0.7104	0.7874	0.5606
GETNext	<u>0.3030</u>	<u>0.6458</u>	<u>0.7561</u>	<u>0.4486</u>	0.4457	0.7610	0.8457	0.5802
MTNet	0.2679	0.5594	0.6692	0.3943	0.4577	0.7321	0.8202	0.5762
TrajGEOS	0.3329	0.6746	0.7755	0.4780	0.4779	0.7201	0.7845	0.5812
TrajGEOS-woGraph	0.3218	0.6584	0.7571	0.4643	0.4683	0.7011	0.7659	0.5678
TrajGEOS-onlyGraph	0.3249	0.6571	0.7560	0.4660	0.4755	0.7138	0.7785	0.5773
TrajGEOS-woShort	0.3150	0.6625	0.7688	0.4605	0.4650	0.7065	0.7750	0.5681
TrajGEOS-woMid	0.3155	0.6600	0.7643	0.4610	0.4749	0.7163	0.7831	0.5780

To further analyze this issue, we increase the number of epochs for TrajGEOS on different datasets and find that the next category prediction task reaches peak performance later than the next location prediction task. Although increasing the number of training epochs can allow TrajGEOS to achieve better results on the next category prediction tasks, it will affect the performance of the next location prediction. Since next location prediction is the main task of this paper, we put priority on optimizing the location prediction task when setting parameters.

B. Performance on different types of locations

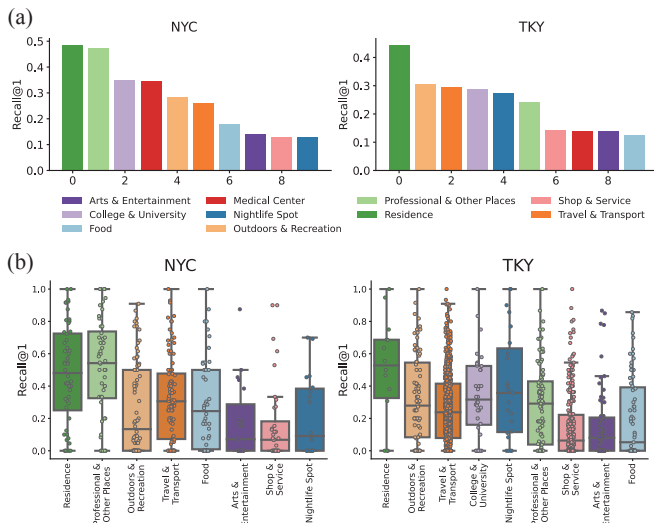


Fig. 6. (a) The average performance of different super-categories. (b) The predicted accuracies of locations in different super-categories.

We check the prediction accuracy for locations that belong to different super-categories in the Foursquare dataset. We first calculate the average prediction accuracies for each super-category and plot them in Figure 6 (a). After calculating the prediction accuracies for every location and categorizing the locations by their super-category, we draw boxplots and strip charts for every super-category as Figure 6 (b) shows. From Figure 6 we find that locations in the ‘Residence’ category are easier to predict. And there are a large number of ‘Travel & Transport’ locations in the TKY dataset, such as ‘Subway’, ‘Train station’, etc., and the processing of this kind of location can be future research content.

C. Sensitivity Analysis

TABLE IV
RESULTS OF DIFFERENT α IN MULTI-TASK LEARNING

α	Category				Location			
	R@1	R@5	R@10	M@10	R@1	R@5	R@10	M@10
0.1	0.3336	0.6782	0.7796	0.4796	0.2619	0.5584	0.6565	0.3857
0.3	0.3348	0.6800	0.7810	0.4809	0.2684	0.5721	0.6692	0.3948
0.5	0.3328	0.6773	0.7781	0.4788	0.2692	0.5733	0.6709	0.3963
0.7	0.3328	0.6745	0.7755	0.4779	0.2721	0.5739	0.6715	0.3982
0.9	0.3283	0.6673	0.7669	0.4722	0.2715	0.5744	0.6717	0.3981

We analyze the influence of hyperparameters α in multi-task learning. Setting different α on the NYC dataset, we get different results like Table IV shows. Table IV shows we can observe that α has an impact on the final results of both category prediction and location prediction. Although the difference in results that have different α is not large, we choose $\alpha = 0.7$ as our optimal parameter based on the evaluation metric *Recall@1* for the next location prediction task.

TABLE V
THE RESULTS OF DIFFERENT LENGTHS OF USER’S RECENT TRAJECTORY ON NYC DATASET

Recent trajectory length (week)	Category				Location			
	R@1	R@5	R@10	M@10	R@1	R@5	R@10	M@10
1	0.3268	0.6672	0.7687	0.4704	0.2682	0.5677	0.6646	0.3930
2	0.3328	0.6745	0.7755	0.4779	0.2721	0.5739	0.6715	0.3982
4	0.3313	0.6794	0.7780	0.4784	0.2712	0.5762	0.6732	0.3986
6	0.3292	0.6783	0.7793	0.4769	0.2713	0.5763	0.6737	0.3987
8	0.3245	0.6773	0.7777	0.4733	0.2675	0.5765	0.6748	0.3968

In addition, we analyze the length of the recent historical trajectory used by our TrajGEOS and set the length of the recent historical trajectory used as 1, 2, 4, 6, and 8 weeks respectively. The prediction results on the NYC dataset are shown in Table V. Based on the *Recall@1* evaluation metric for the next location prediction task, we finally choose to use the user’s historical trajectory from the past two weeks for both modeling and forecasting.

D. The effectiveness of orientation module

To explain why we use the Orientation module instead of directly using GRU to learn user mid-term preferences, we replace the Orientation module in TrajGEOS with GRU to process the recent trajectory information, and the output is used as the initial state to process the GRU of the current trajectory. The results obtained by setting different lengths of the recent sub-trajectories utilized to calculate the user’s mid-term preference are shown in Table VI.

TABLE VI
REPLACE THE ORIENTATION MODULE WITH GRU AND CHECK ITS PERFORMANCE ON THE NYC DATASET WITH DIFFERENT LENGTHS OF SUB-TRAJECTORIES THAT COMPOSE THE RECENT TRAJECTORIES. EVERY RECENT SUB-TRAJECTORY IS THE TRACE OF A USER IN A WEEK.

Num of recent sub-trajectories	Category				Location			
	R@1	R@5	R@10	M@10	R@1	R@5	R@10	M@10
1	0.3238	0.6670	0.7682	0.4683	0.2636	0.5697	0.6688	0.3913
2	0.3257	0.6690	0.7708	0.4706	0.2655	0.5721	0.6714	0.3934
4	0.3259	0.6702	0.7716	0.4707	0.2651	0.5714	0.6704	0.3925
6	0.3272	0.6714	0.7728	0.4726	0.2667	0.5717	0.6703	0.3937
8	0.3262	0.6711	0.7704	0.4712	0.2649	0.5709	0.6696	0.3920

E. Different number of EGraphSAGE layers on global trajectory graph

To determine the optimal number of graph convolution layers on the global trajectory graph, we conducted experiments on the NYC dataset. We first set the number of convolution layers on the user trajectory subgraph to 2, and then tested 2, 3, 4, and 5 graph convolution layers on the global graph, respectively. The experimental results are shown in Table VII. Based on the *Recall@1* metric of the next place prediction task, we finally use 2-layer graph convolutions to generate the embedding of nodes on the global trajectory graph.

TABLE VII

RESULT ON NYC DATASET WITH DIFFERENT EGRAPH SAGE LAYER NUMS ON GLOBAL TRAJECTORY GRAPH

EGraphSAGE Layer Num	Category				Location			
	R@1	R@5	R@10	M@10	R@1	R@5	R@10	M@10
2	0.3329	0.6746	0.7755	0.4780	0.2721	0.5740	0.6716	0.3982
3	0.3324	0.6768	0.7765	0.4779	0.2709	0.5740	0.6709	0.3974
4	0.3314	0.6766	0.7743	0.4772	0.2704	0.5741	0.6710	0.3973
5	0.3326	0.6756	0.7752	0.4774	0.2715	0.5730	0.6708	0.3973

F. Different number of GraphSAGE layers on user's trajectory graph

Under the condition of utilizing two global graph convolutional layers, we further investigate the impact of using different numbers of graph convolutional layers for subgraph links in user trajectories on experimental outcomes. We conduct experiments on the NYC dataset and present our findings in Table A. Based on the *Recall@1* metric for the next place prediction task, we finally employ a 2-layer GraphSAGE for graph learning on user trajectory graphs.

TABLE VIII

RESULT ON NYC DATASET WITH DIFFERENT GRAPH S AGE LAYER NUMS ON USER'S TRAJECTORY GRAPH

GraphSAGE Layer Num	Category				Location			
	R@1	R@5	R@10	M@10	R@1	R@5	R@10	M@10
2	0.3329	0.6746	0.7755	0.4780	0.2721	0.5740	0.6716	0.3982
3	0.3283	0.6680	0.7666	0.4725	0.2716	0.5722	0.6694	0.3975
4	0.3281	0.6673	0.7660	0.4722	0.2718	0.5724	0.6681	0.3971
5	0.3258	0.6617	0.7630	0.4686	0.2708	0.5720	0.6677	0.3963

REFERENCES

- [1] Y. Xu and M. C. González, "Collective benefits in traffic during mega events via the use of information technologies," *Journal of The Royal Society Interface*, vol. 14, no. 129, p. 20161041, 2017.
- [2] S. Çolak, A. Lima, and M. C. González, "Understanding congested travel in urban areas," *Nature communications*, vol. 7, no. 1, p. 10793, 2016.
- [3] Y. Xu, S. Çolak, E. C. Kara, S. J. Moura, and M. C. González, "Planning for electric vehicle needs by coupling charging profiles with urban mobility," *Nature Energy*, vol. 3, no. 6, pp. 484–493, 2018.
- [4] E. Barbour, C. C. Davila, S. Gupta, C. Reinhart, J. Kaur, and M. C. González, "Planning for sustainable cities by estimating building occupancy with mobile phones," *Nature communications*, vol. 10, no. 1, p. 3736, 2019.
- [5] F. Xu, Y. Li, D. Jin, J. Lu, and C. Song, "Emergence of urban growth patterns from human mobility behavior," *Nature Computational Science*, vol. 1, no. 12, pp. 791–800, 2021.
- [6] T. Yabe, N. K. Jones, P. S. C. Rao, M. C. Gonzalez, and S. V. Ukkusuri, "Mobile phone location data for disasters: A review from natural hazards and epidemics," *Computers, Environment and Urban Systems*, vol. 94, p. 101777, 2022.
- [7] C. Song, Z. Qu, N. Blumm, and A.-L. Barabási, "Limits of predictability in human mobility," *Science*, vol. 327, no. 5968, pp. 1018–1021, 2010.
- [8] Y. Xu, R. D. Clemente, and M. C. González, "Understanding vehicular routing behavior with location-based service data," *EPJ Data Science*, vol. 10, no. 1, pp. 1–17, 2021.
- [9] D. Yang, D. Zhang, V. W. Zheng, and Z. Yu, "Modeling user activity preference by leveraging user spatial temporal characteristics in lbsns," *IEEE Transactions on Systems, Man, and Cybernetics: Systems*, vol. 45, no. 1, pp. 129–142, 2014.
- [10] Y. Tang, J. He, and Z. Zhao, "Hgarn: Hierarchical graph attention recurrent network for human mobility prediction," *arXiv preprint arXiv:2210.07765*, 2022.
- [11] P. Zhao, A. Luo, Y. Liu, J. Xu, Z. Li, F. Zhuang, V. S. Sheng, and X. Zhou, "Where to go next: A spatio-temporal gated network for next poi recommendation," *IEEE Transactions on Knowledge and Data Engineering*, vol. 34, no. 5, pp. 2512–2524, 2020.
- [12] Q. Liu, S. Wu, L. Wang, and T. Tan, "Predicting the next location: A recurrent model with spatial and temporal contexts," in *Thirtieth AAAI conference on artificial intelligence*, 2016.
- [13] D. Yang, B. Fankhauser, P. Rosso, and P. Cudre-Mauroux, "Location prediction over sparse user mobility traces using rnns," in *Proceedings of the Twenty-Ninth International Joint Conference on Artificial Intelligence*, 2020, pp. 2184–2190.
- [14] D. Kong and F. Wu, "Hst-lstm: A hierarchical spatial-temporal long-short term memory network for location prediction," in *IJCAI*, vol. 18, no. 7, 2018, pp. 2341–2347.
- [15] J. Manotumruksa, C. Macdonald, and I. Ounis, "A contextual attention recurrent architecture for context-aware venue recommendation," in *The 41st international ACM SIGIR conference on research & development in information retrieval*, 2018, pp. 555–564.
- [16] Y. Chen, C. Long, G. Cong, and C. Li, "Context-aware deep model for joint mobility and time prediction," in *Proceedings of the 13th International Conference on Web Search and Data Mining*, 2020, pp. 106–114.
- [17] J. Feng, Y. Li, C. Zhang, F. Sun, F. Meng, A. Guo, and D. Jin, "Deep-move: Predicting human mobility with attentional recurrent networks," in *Proceedings of the 2018 world wide web conference*, 2018, pp. 1459–1468.
- [18] Y. Luo, Q. Liu, and Z. Liu, "Stan: Spatio-temporal attention network for next location recommendation," in *Proceedings of the Web Conference 2021*, 2021, pp. 2177–2185.
- [19] S. Yang, J. Liu, and K. Zhao, "Getnext: trajectory flow map enhanced transformer for next poi recommendation," in *Proceedings of the 45th International ACM SIGIR Conference on research and development in information retrieval*, 2022, pp. 1144–1153.
- [20] Y. Hong, H. Martin, and M. Raubal, "How do you go where? improving next location prediction by learning travel mode information using transformers," in *Proceedings of the 30th International Conference on Advances in Geographic Information Systems*, 2022, pp. 1–10.
- [21] H. Xue, F. Salim, Y. Ren, and N. Oliver, "Mobtcast: Leveraging auxiliary trajectory forecasting for human mobility prediction," *Advances in Neural Information Processing Systems*, vol. 34, pp. 30380–30391, 2021.
- [22] S. Rendle, C. Freudenthaler, and L. Schmidt-Thieme, "Factorizing personalized markov chains for next-basket recommendation," in *Proceedings of the 19th international conference on World wide web*, 2010, pp. 811–820.
- [23] C. Cheng, H. Yang, M. R. Lyu, and I. King, "Where you like to go next: Successive point-of-interest recommendation," in *Twenty-Third international joint conference on Artificial Intelligence*, 2013.
- [24] M. Ye, P. Yin, W.-C. Lee, and D.-L. Lee, "Exploiting geographical influence for collaborative point-of-interest recommendation," in *Proceedings of the 34th international ACM SIGIR conference on Research and development in Information Retrieval*, 2011, pp. 325–334.
- [25] C. Cheng, H. Yang, I. King, and M. Lyu, "Fused matrix factorization with geographical and social influence in location-based social networks," in *Proceedings of the AAAI conference on artificial intelligence*, vol. 26, no. 1, 2012, pp. 17–23.
- [26] X. Li, G. Cong, X.-L. Li, T.-A. N. Pham, and S. Krishnaswamy, "Rank-geofm: A ranking based geographical factorization method for point of interest recommendation," in *Proceedings of the 38th international ACM SIGIR conference on research and development in information retrieval*, 2015, pp. 433–442.
- [27] D. Lian, C. Zhao, X. Xie, G. Sun, E. Chen, and Y. Rui, "Geomf: joint geographical modeling and matrix factorization for point-of-interest recommendation," in *Proceedings of the 20th ACM SIGKDD international conference on Knowledge discovery and data mining*, 2014, pp. 831–840.

- [28] S. Feng, X. Li, Y. Zeng, G. Cong, Y. M. Chee, and Q. Yuan, "Personalized ranking metric embedding for next new poi recommendation," in *Twenty-Fourth International Joint Conference on Artificial Intelligence*, 2015.
- [29] S. Feng, L. V. Tran, G. Cong, L. Chen, J. Li, and F. Li, "Hme: A hyperbolic metric embedding approach for next-poi recommendation," in *Proceedings of the 43rd International ACM SIGIR Conference on Research and Development in Information Retrieval*, 2020, pp. 1429–1438.
- [30] S. Zhao, T. Zhao, H. Yang, M. R. Lyu, and I. King, "Stellar: Spatial-temporal latent ranking for successive point-of-interest recommendation," in *Thirtieth AAAI conference on artificial intelligence*, 2016.
- [31] Y. Wu, K. Li, G. Zhao, and X. Qian, "Long-and short-term preference learning for next poi recommendation," in *Proceedings of the 28th ACM international conference on information and knowledge management*, 2019, pp. 2301–2304.
- [32] D. Lian, Y. Wu, Y. Ge, X. Xie, and E. Chen, "Geography-aware sequential location recommendation," in *Proceedings of the 26th ACM SIGKDD international conference on knowledge discovery & data mining*, 2020, pp. 2009–2019.
- [33] K. Sun, T. Qian, T. Chen, Y. Liang, Q. V. H. Nguyen, and H. Yin, "Where to go next: Modeling long-and short-term user preferences for point-of-interest recommendation," in *Proceedings of the AAAI Conference on Artificial Intelligence*, vol. 34, no. 01, 2020, pp. 214–221.
- [34] Y. Wu, K. Li, G. Zhao, and Q. Xueming, "Personalized long-and short-term preference learning for next poi recommendation," *IEEE Transactions on Knowledge and Data Engineering*, 2020.
- [35] Y. Qin, C. Gao, Y. Wang, S. Wei, D. Jin, J. Yuan, and L. Zhang, "Disentangling geographical effect for point-of-interest recommendation," *IEEE Transactions on Knowledge and Data Engineering*, vol. 35, no. 8, pp. 7883–7897, 2022.
- [36] Q. Gao, J. Hong, X. Xu, P. Kuang, F. Zhou, and G. Trajcevski, "Predicting human mobility via self-supervised disentanglement learning," *IEEE Transactions on Knowledge and Data Engineering*, 2023.
- [37] Z. Huang, S. Xu, M. Wang, H. Wu, Y. Xu, and Y. Jin, "Human mobility prediction with causal and spatial-constrained multi-task network," *EPJ Data Science*, vol. 13, no. 1, p. 22, 2024.
- [38] M. Xie, H. Yin, H. Wang, F. Xu, W. Chen, and S. Wang, "Learning graph-based poi embedding for location-based recommendation," in *Proceedings of the 25th ACM international on conference on information and knowledge management*, 2016, pp. 15–24.
- [39] X. Xiong, F. Xiong, J. Zhao, S. Qiao, Y. Li, and Y. Zhao, "Dynamic discovery of favorite locations in spatio-temporal social networks," *Information Processing & Management*, vol. 57, no. 6, p. 102337, 2020.
- [40] A. Vaswani, N. Shazeer, N. Parmar, J. Uszkoreit, L. Jones, A. N. Gomez, E. Kaiser, and I. Polosukhin, "Attention is all you need," *Advances in neural information processing systems*, vol. 30, 2017.
- [41] X. Rao, L. Chen, Y. Liu, S. Shang, B. Yao, and P. Han, "Graph-flashback network for next location recommendation," in *Proceedings of the 28th ACM SIGKDD conference on knowledge discovery and data mining*, 2022, pp. 1463–1471.
- [42] X. Yan, T. Song, Y. Jiao, J. He, J. Wang, R. Li, and W. Chu, "Spatio-temporal hypergraph learning for next poi recommendation," in *Proceedings of the 46th international ACM SIGIR conference on research and development in information retrieval*, 2023, pp. 403–412.
- [43] T. Huang, X. Pan, X. Cai, Y. Zhang, and X. Yuan, "Learning time slot preferences via mobility tree for next poi recommendation," in *Proceedings of the AAAI Conference on Artificial Intelligence*, vol. 38, no. 8, 2024, pp. 8535–8543.
- [44] J. You, X. Ma, Y. Ding, M. J. Kochenderfer, and J. Leskovec, "Handling missing data with graph representation learning," *Advances in Neural Information Processing Systems*, vol. 33, pp. 19 075–19 087, 2020.
- [45] W. Hamilton, Z. Ying, and J. Leskovec, "Inductive representation learning on large graphs," *Advances in neural information processing systems*, vol. 30, 2017.
- [46] S. M. Kazemi, R. Goel, S. Eghbali, J. Ramanan, J. Sahota, S. Thakur, S. Wu, C. Smyth, P. Poupart, and M. Brubaker, "Time2vec: Learning a vector representation of time," *arXiv preprint arXiv:1907.05321*, 2019.
- [47] E. Cho, S. A. Myers, and J. Leskovec, "Friendship and mobility: user movement in location-based social networks," in *Proceedings of the 17th ACM SIGKDD international conference on Knowledge discovery and data mining*, 2011, pp. 1082–1090.